An Image-Based Multi-Directional Reflectance Measurement Setup for Flexible Objects

Aditya S. Sole[a], Ivar Farup[a] and Shoji Tominaga[b]

[a]The Norwegian Colour and Visual Computing Laboratory, Gjøvik University College, Gjøvik, Norway;

[b]Graduate School of Advanced Integration Science, Chiba University, Chiba, Japan

ABSTRACT

This paper presents an image-based method to measure reflectance of a homogeneous flexible object material (usually used in packaging). A point light source and a commercially available RGB camera is used to illuminate and measure the radiance reflected from the object surface in multiple reflection directions. By curving the flexible object onto a cylinder of known radius we are able to record radiance at multiple reflection angles in a faster way. In order to estimate the reflectance and to characterise the material, a spectralon reference tile is used. The spectralon tile is assumed to be homogenous and has near lambertain surface properties. Using Lambert's cosine law, irradiance at a given point on the object surface is calculated. This information is then used to calculate a BRDF using Phong reflection model to describe the sample surface reflection properties. The measurement setup is described and discussed in this paper along with its use to estimate a BRDF for a given material/substrate. Results obtained indicate that the proposed image-based technique works well to measure light reflected at different planar angles and record information to estimate the BRDF of the sample materials that can be modelled using Phong reflection model. The object material properties, sample curvature and camera resolution decides the number of incident and reflection angles at which the bi-directional reflectance, or the material BRDF, can be estimated using this method.

Keywords: BRDF, Phong model, multi-angle reflection measurement, goniometric measurements

1. INTRODUCTION

Appearance of an object material is measured with the goal of objectively describing and quantifying human visual impressions with measurement values. Measurements help us communicate the appearance of the material in numerical terms. Material appearance can be described using surface reflectance properties. A Bidirectional Reflection Distribution Function (BRDF) of material will describe the surface reflectance properties of that material. BRDF completely describes the reflectance of an opaque surface at a given point.[1] The most appropriate way to measure the surface reflectance is by performing physical measurements of the reflected light.[1]

Physical reflectance measurements are performed (for example, in the packaging and car paint industry) to characterise and control reproduction of materials like printed packages and paints.[2,3] Different surface properties of these materials help produce desirable appearance of the material that varies with the direction of illumination and viewing. Many car paints used in car industry or gonio-chromatic materials used in print and packaging industry[2,4] produce a very desirable appearance by showing a shift or change in perceived colour depending upon illumination and viewing geometry. This change is achieved due to varying reflection at different viewing angles. Studies have shown that flexible materials like paper substrates (typically used in print and packaging industry) reflects light in an anisotropic manner.[5,6] The reflected light quantity is therefore dependent on incident light and viewing directions.

These substrates should therefore be measured with instrument measuring at more than one illumination and reflection angle combination[2,7] unlike the single geometry instruments (for example $0°$:$45°$) traditionally used in

Further author information: (Send correspondence to Aditya S. Sole)
Aditya S. Sole: E-mail: adityas@hig.no, adityasole@gmail.com, Telephone: +47 611 35168
Ivar Farup: E-mail: ivar.farup@hig.no, Telephone: +47 611 35227
Shoji Tominaga: E-mail: shoji@faculty.chiba-u.jp, Telephone: +81 (0)90 2197 0543

Measuring, Modeling, and Reproducing Material Appearance 2015, edited by Maria V. Ortiz Segovia, Philipp Urban, Francisco H. Imai, Proc. of SPIE-IS&T Vol. 9398, 93980J · © 2015 SPIE-IS&T · CCC code: 0277-786X/15/$18 · doi: 10.1117/12.2076592

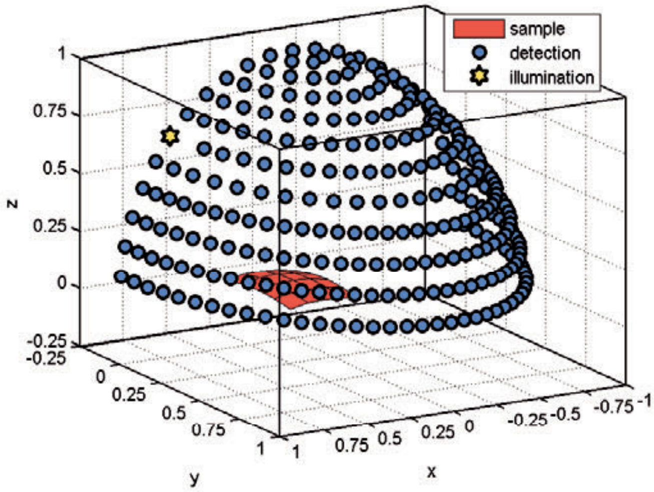

Figure 1: Gonio-metric measurements (Image taken from[3] and is licensed under CC BY-NC-ND).

the graphic arts and textile industry. Several commercial instruments available in the market (for example, X-rite MA98, BYK-Mac) can be used to perform multi-angle planar measurements. These instruments, however, are expensive and measure at a fixed illumination and reflection angles.[8] Gonio-spectro-photometers (mainly used in metrology institutes and research laboratories) can also be used to perform multi-angle plannar measurements. These instruments are more accurate and also measure gonio-metrically (refer figure 1). However, gonio-spectro-photometers are expensive and slow. There is, therefore a clear need to cover the bridge between the accurate (but slow) metrological instruments (like gonio-spectro-photometers) and user centric measurement methods/setups which should be fast and inexpensive.

In this paper we present an image based measurement setup, similar to ones proposed and used in measurement of velvets,[9] gloss[10] and human skin measurement,[1] to measure such materials at a faster speed. The measurement setup uses a point light source and a commercially available digital camera sensor (for example Nikon D200 DSLR camera) along with the sample to be measured. In the existing measurement setups (e.g. gonio-spectrometers, multi-angle spectrophotometers), the sample is usually flat on a surface and the light capturing sensor and/or light source rotate/move in the planar angles and azimuthal directions to illuminate and record the reflected light from the sample surface in different directions.[3] These setups therefore require considerable amount of time to record the reflectance at multiple angles. In order to avoid these moving parts (which are main cause of increase in measurement time) and thus reduce the measurement time, in the proposed setup, we keep the light source and the measurement sensor at fixed position from the sample (for example light source at 45° and sensor at 0°) and curve the measurement sample onto a cylinder[1,9–11] as shown in figure 2.

2. MEASUREMENT SETUP

Figure 2[12] shows the measurement setup we use for capturing the light reflected from a material substrate using an image based device. We, therefore, replace the flat surface measurement (using gonio-spectrometer) with a curved surface observation by a camera in our setup. The semi-circle (S) will be the curved substrate (for example packaging sample print) to be measured. The substrate is curved onto a cylinder of known radius (R). Point (C) is the sensor position (digital camera sensor) approximately at the center of the curved sample at a fixed distance d_C. L is a point light source illuminating the sample at a fixed angle $0^\circ < \theta_L < 90^\circ$ at a known distance d_L from the center of the curved sample.

Assuming that the curved sample is homogeneous, light incident and reflected at any given point on the sample will provide information with respect to the light source position (L), camera (C) and the surface normal vector ($\mathbf{n}$) direction. Figure 2 also shows the setup in a vector plane were θ_i and θ_r are incident and reflection

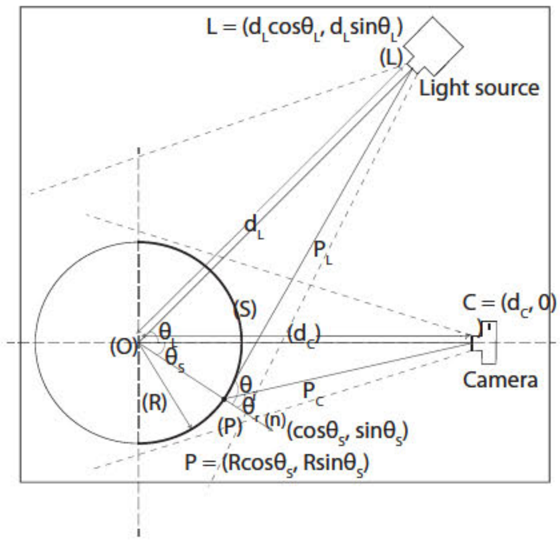

Figure 2: Measurement setup.

Table 1: θ_S calculation error.

Ruler points (*angles* °)	-40	-30	-20	-10	0	10	20	30	40
Calculated angles (*angles* °)	-41.90	-31.99	-22.05	-12.07	-2.12	7.7	17.7	27.68	37.7

angles with respect to the normal n at a given point P on the curved sample surface. Incident θ_i and reflection θ_r angles can be calculated as,[12]

$$\cos\theta_i = \frac{\mathbf{P}_L \cdot \mathbf{n}}{\mid P_L \mid} = \frac{d_L \cos(\theta_L - \theta_S) - R}{\sqrt{d_L^2 + R^2 - 2d_L R \cos(\theta_L - \theta_S)}},$$
$$\cos\theta_r = \frac{\mathbf{P}_C \cdot \mathbf{n}}{\mid P_C \mid} = \frac{d_C \cos\theta_S - R}{\sqrt{d_C^2 + R^2 - 2d_C R \cos\theta_S}}. \quad (1)$$

From Equation (1) it can be observed that when choosing a point on the curved sample surface to record the incident and reflected light, the θ_S angle changes with change in the location on the curved surface. θ_S can therefore be calculated using,[12]

$$\cos\theta_S = \frac{2d_C R d_A^2 \pm \sqrt{\left(-2d_C R d_A^2\right)^2 - 4\left(R^2 d_A^2 + F_L^2 R^2\right)\left(d_C^2 d_A^2 - F_L^2 R^2\right)}}{2R^2\left(d_A^2 + F_L^2\right)}. \quad (2)$$

In order to verify the θ_S calculation, an angular ruler was printed on a white paper substrate and measured using the setup. Figure 3 shows the captured image. The angular ruler can be observed at the bottom of the curved scene. The ruler points on the printed angular ruler indicate the θ_S angles, the corresponding pixel positions on the camera sensor, should measure/calculate using the Equation (1).[12] In order to minimize distortion due to lens, the object is positioned at the center of the image plane with sufficient distance from all the 4 corners. Unlike Marschner's[1] method, we perform manual physical measurements to determine the incident light position and camera. The pixel points corresponding to the angular ruler are located using second derivative[12] and the corresponding θ_S are calculated using Equation (2). Table 1 shows the calculated θ_S and the angular ruler points. We can observe an average error of 2.13 ° when calculating the reflection angles using Equation (2).[12] Figure 4 shows the error against the ruler points. The error can be corrected either by physically rotating the sample or subtracting the average error obtained from the calculated θ_S. For further calculation using θ_S the

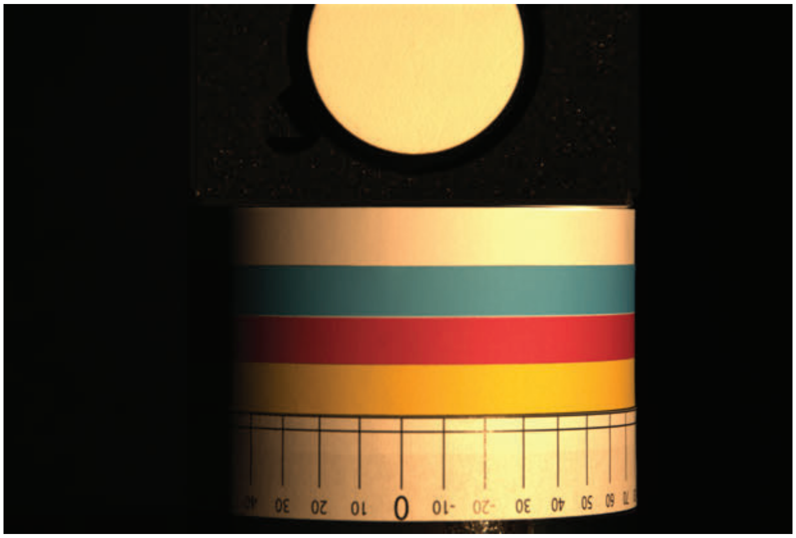

Figure 3: Captured image.

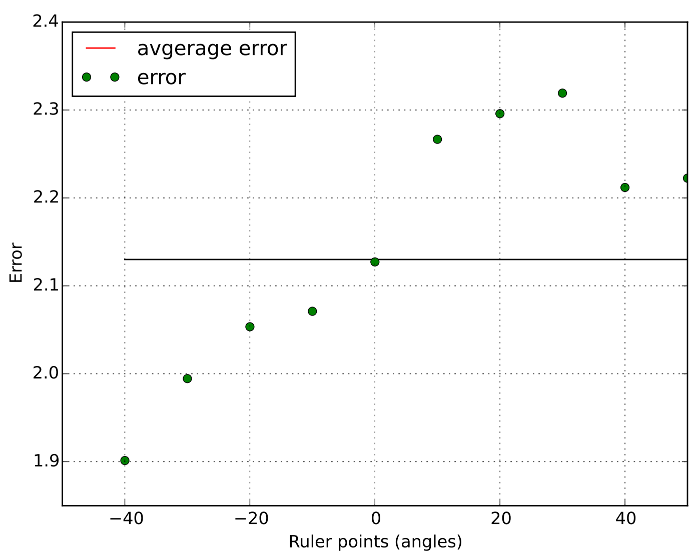

Figure 4: θ_S calculation error.

average error was subtracted from the calculated θ_S for the corresponding pixel points in the captured image. This corrected θ_S value was used for calculating θ_r and θ_r angles using Equation (1).

3. SAMPLE MEASUREMENT

A diffuse packaging print sheet (Matt coated white plotter sheet) was printed with solid colour patches to measure with the setup. Cyan and magenta colour patches were measured along with the paper white. These three materials are referred as material C (Cyan), M (Magenta) and W (Paper white) in the paper from here on. The sheet was wrapped around a cylinder of known radius (R=56mm). The image was captured using a Nikon D200 digital camera from a fixed distance (Cl=630mm). The curved sample on the cylinder was illuminated using a point light source at a distance (dL= approx. 1922mm). Figure (3) shows the captured image. The scene/curved sample was measured at three incident light directions (θ_L=29°, 39° and 47°). Spectralon tile was used as a reference to estimate the light incident on the curved sample and to normalise the image data.

The number of reflection angles at which the reflection information is to be recorded depends on the sample curvature.[12] As the curved sample is illuminated using a point light source at an incident light angle of θ_L=29°, 39°, 47° the illuminated areas on the curved sample is different for different θ_L. Therefore a part (horizontal) of the curved sample which is uniformly illuminated at all three incident (θ_L) angles is considered for the measurements.

Reference white measurement were recorded using the spectralon tile approximtely at θ_r=0°. For each respective measurement, average of 100 pixel lines (along vertical axis) was used as the respective measurement.

Amount of light incident on the curved sample was calculated using the spectralon tile measurements. Assuming spectralon tile as lambertian we measure the light intensity at θ_r=0° on the spectralon tile (θ_i=θ_L). Using lambert's cosine law we estimate the light incident on the curved sample,

$$\begin{aligned} I_r &= I_i \cos\theta_i \\ I_i &= \frac{I_r}{\cos\theta_i} \end{aligned} \tag{3}$$

Where, I_i is the light incident on the sample, I_r is the amount of light reflected from the reference white tile (spectralon tile) and θ_i is the angle between point on the reference tile and incident light direction (θ_L).

4. BRDF CALCULATION USING PHONG REFLECTION MODEL

Bi-directional reflection distribution function (BRDF) describes the surface reflectance properties of a given opaque material.[13] The BRDF is defined[13] by,

$$f_r(\theta_i, \phi_i, \theta_r, \phi_r) = \frac{dL_r(\theta_i, \phi_i, \theta_r, \phi_r, E_i)}{dE_i(\theta_i, \phi_r)} \tag{4}$$

i and r denote incidence and reflection respectively. θ and ϕ together indicate the direction, E_i is incident irradiance, L_r is reflectance radiance and d is the differential quantity.

Modelling the reflection properties of material surfaces is important for material appearance measurement and simulation. Reflection models are widely used in computer graphics for generating realistic images.[14–16] In print and packaging applications, a reflectance model can be used for simulating the colour reproduction process.

The packaging print sheet printed with Magenta and Cyan solid inks showed fairly diffuse reflection properties with small amount of specular reflection on visual inspection. Phong reflection model was used to calculate the BRDF of these three material surfaces (materials C, M and W). Phong reflection model is an empirical model with two surface reflection components, diffuse reflection of rough surfaces and specular reflection of shiny surfaces.[14] Figure 5 shows the reflection geometry used for the Phong model, where **N** is the surface normal, **L** is the incident light vector, and **V** is the viewing vector. **R** and **Rv** are, respectively, **L** and **V** mirrored about **N**. A three-dimensional light reflection of the Phong model can be described[17] as

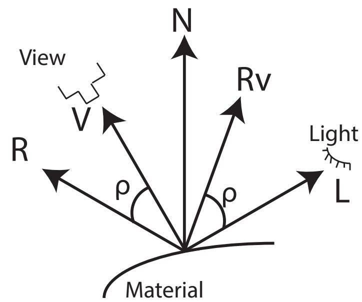

Figure 5: Vector diagram for Phong reflection model calculation.

$$Y(\theta, \lambda) = E_{amb}(\lambda) + (\cos\phi)\, S_d(\lambda)\, E(\lambda) + (\cos^{\alpha}\rho)\, S_s E(\lambda) \tag{5}$$

$Y(\theta, \lambda)$ is the radiance of light reflected from a surface and is a function of wavelenght (λ) and the geometric parameter θ, including the illumination direction angle, the viewing angle, and the phase angle. E_{amb} is the ambient light, $S_d(\lambda)$ is the surface-spectral reflectance of an object surface and $E(\lambda)$ is the spectral power distribution of the incident light. ϕ is the angle of incidence, ρ is the angle between the viewing vector $\mathbf{V}$ and the mirrored vector $\mathbf{R}$ of incident light vector (refer Figure 5), α is used as the measure of surface roughness and S_s is a constant value. The Phong model can be used with the measurement setup by inserting the model parameters with respect to the measurement setup. Referring Figure 2

$$\begin{aligned} \cos\phi &= \cos\theta_i \\ \cos^{\alpha}\rho &= \cos^{\alpha}(\theta_r - \theta_i) \end{aligned} \tag{6}$$

As the measurements were recorded using a colour camera. The camera output can be described as

$$\begin{bmatrix} R \\ G \\ B \end{bmatrix} = \int_{400}^{700} Y(\theta, \lambda) \begin{bmatrix} r(\lambda) \\ g(\lambda) \\ b(\lambda) \end{bmatrix} d\lambda \tag{7}$$

where $r(\lambda)$, $g(\lambda)$ and $b(\lambda)$ are the spectral sensitivity functions of the camera. Inserting Equation (6) in Equation (5), the camera colour output I at the spatial location p can be described as

$$I_p = \begin{bmatrix} R \\ G \\ B \end{bmatrix} = k_a \mathbf{I_a} + k_d \mathbf{I_d}(\cos\theta_i) + k_s \mathbf{I_s}(\cos^{\alpha}(\theta_r - \theta_i)). \tag{8}$$

$\mathbf{I_a}$ is the ambient light vectors, $\mathbf{I_d}$ is the diffuse component (object colour) vectors, $\mathbf{I_s}$ is the specular component (incident light) vectors. k_a, k_d, k_s, are the ambient, diffuse and specular reflection constants.

4.1 Colour Phong reflection model

In this paper we implement the Phong model using two methods. In the *first method* - Colour Phong reflection model, we use the object colour vector (body reflection) as the diffuse component $\mathbf{I_d}$ and the incident light as the specular component as defined in Equation (8). Diffuse component $(\mathbf{I_d})$ value for each material was selected from the non-specular region of the captured image. From the calculated incident and reflection angles and the known incident light direction (θ_L) an approximate pixel area (average of 2500 pixels) was selected from the non-specular area of the image. Specular component is the light incident $(\mathbf{I_i})$ on the material. Table 2 below shows the I_d value for each material (W,C and M). The ambient light term is treated as a constant $K_a\mathbf{I_a}$=k_{amb}. Equation (8) therefore can be written as

$$I_p = k_{amb} + k_d \begin{bmatrix} R^0 \\ G^0 \\ B^0 \end{bmatrix} cos\theta_i + k_s \mathbf{I_i}(\cos^{\alpha}(\theta_r - \theta_i)). \tag{9}$$

Table 2: Material body reflection component (I_d).

Material	Red (R^0)	Green (G^0)	Blue (B^0)
W	0.7612	0.5458	0.3500
C	0.3962	0.6601	0.6381
M	0.9473	0.2321	0.2204

Table 3: Phong model parameters fitted using Colour Phong reflection model (Section 4.1).

Material	ka	kd	ks	alpha	LRMSE
W	0.0566	0.5493	0.1691	0.8339	0.0193
C	0.0265	0.3307	0.0760	1.2109	0.0170
M	0.0034	0.4242	0.0785	0.8681	0.0174

$[R^0, G^0, B^0]^T$ is the normalised object body reflection (refer Table 2) of the respective material (W, C, M) and $\mathbf{I_i}$ is an identity vector $[1, 1, 1]^T$. We use Equation (9) as a color model for the Phong reflection model. Reflection constants (k_{amb}, k_d, k_s and α) were therefore fitted in Equation (9) using the data captured at three incident light directions (θ_L=29 °, 39 °, 47 °) and R, G and B sensors for the respective materials. The constants were further optimized using the Nelder-Mead downhill simplex algorithm[18] to find the minimum of a function with the given paramters. Root mean square (RMS) error between the measured data and the estimated data was used as the minimizing function. Table 3 shows the reflection constant fitted for the three materials (C, M and W) using Equation (9). Figures (6,7, and 8) shows the plots for the light intensity reflected from the three materials (C, M and W) and the light intensity estimated using Equation (9) for 2 incident light directions (θ_L=29 ,θ_L=47).

4.2 Monochrome Phong reflection model

As we have used a point light source and the materials measured using the setup being fairly diffuse, in the *second method* - Monochrome Phong reflection model, we use the incident light I_i in all the three components of the model. That is I_a=I_d=I_s=I_i. Also the ambient light term is treated as a constant $K_a I_i$=k_{amb}. Inserting this in Equation (8),

$$I_p = k_{amb} + I_i(k_d(\cos\theta_i) + k_s(\cos^\alpha(\theta_r - \theta_i)). \quad (10)$$

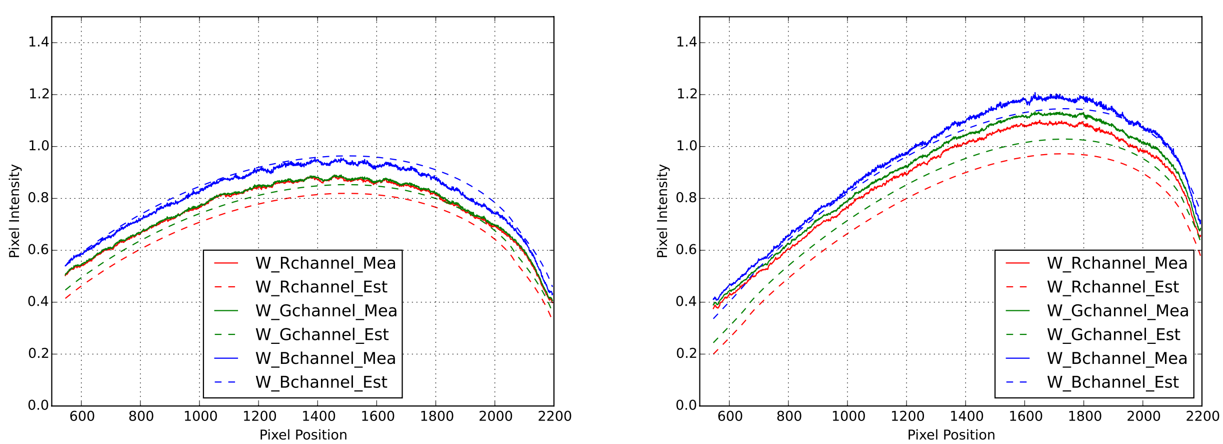

(a) θ_L=29 °

(b) θ_L=47 °

Figure 6: Reflected intensity I_p measured and estimated using Equation (9) for material W.

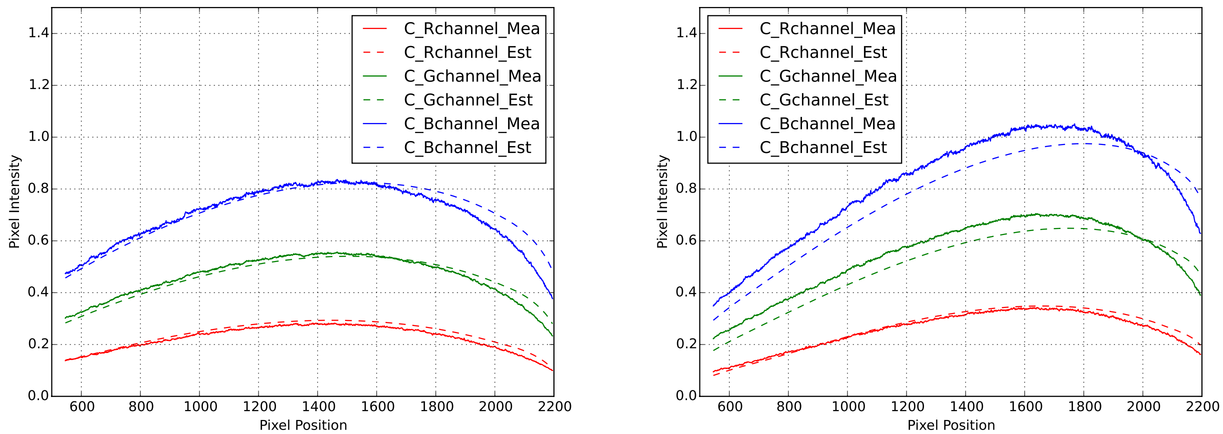

(a) θ_L=29° (b) θ_L=47°

Figure 7: Reflected intensity I_p measured and estimated using Equation (9) for material C.

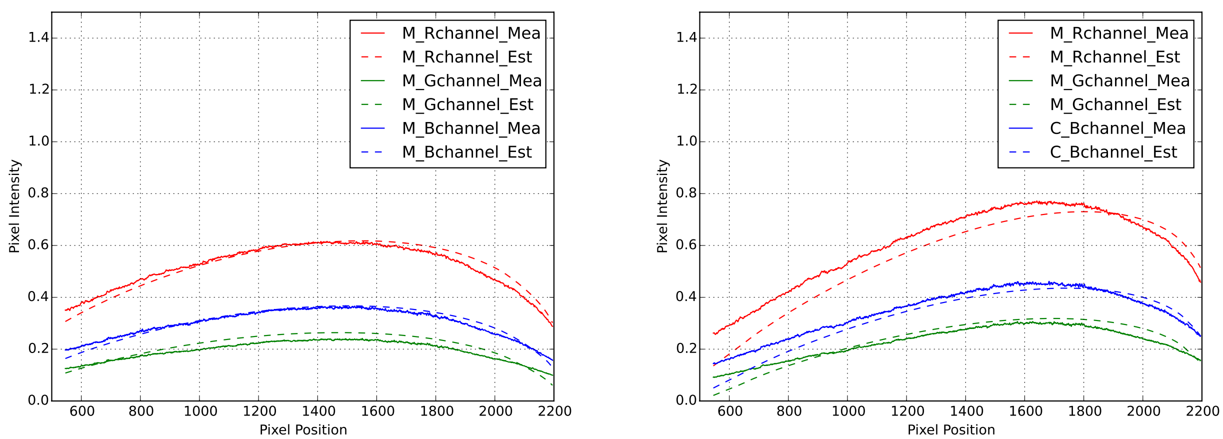

(a) θ_L=29° (b) θ_L=47°

Figure 8: Reflected intensity I_p measured and estimated using Equation (9) for material M.

As the image is captured using an RGB sensor camera, in this method we model the above Equation (refer Equation 10) separately for R, G and B intensities, thus having different reflection constants k_{amb}, k_d, k_s and α for individual R, G and B sensor channels for the respective materials.

The reflection constants k_{amb}, k_d, k_s and α were fitted in Equation (10) using the data captured at three incident light directions (θ_L=29°, 39°, 47°) for the materials W, C and M. Similar to the Colour model (refer Section 4.1), the constants were further optimized the Nelder-Mead downhill simplex algorithm.[18] Root mean square (RMS) error between the measured data and the estimated data (using Equation (10) was used as the minimizing function. Table 4 shows the reflection constants fitted for the three materials (C, M and W) for individual sensor channels (R,G,B) using the data captured with three different incident light directions (θ_L=29°, 39°, 47°). Figures 9,10, and 11 show the plots for the light intensity reflected from the three materials (C, M and W) and the light intensity estimated using the above model for the three sensor channels (R, G, B) and for 2 incident light directions (θ_L=29 , θ_L=47). We believe that modelling the Phong parameters for individual sensors (R, G and B in this case) should help us simulate the material appearance with more control for highly specular and gonio-chromatic colours. Phong parameters of individual sensors should help simulate the gonio-chromatic appearance of homogenous material once the incident light intensity (I_i), direction (θ_L) and

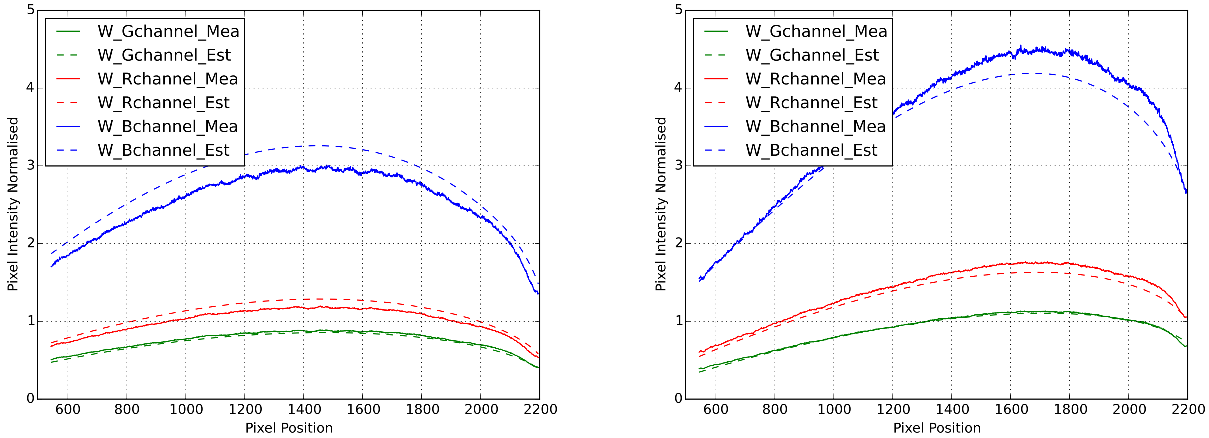

(a) θ_L=29° (b) θ_L=47°

Figure 9: Reflected intensity I_p measured and estimated using Equation (10) for material W.

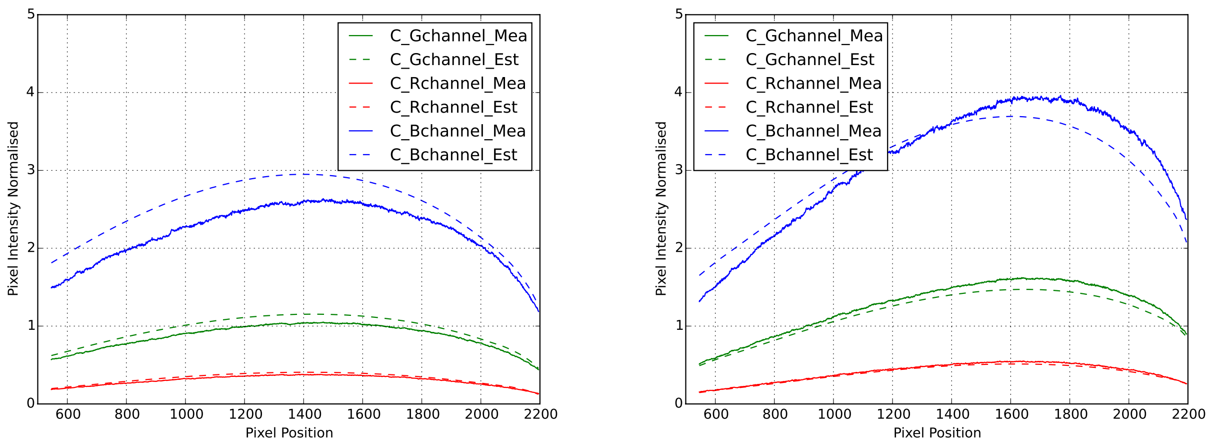

(a) θ_L=29° (b) θ_L=47°

Figure 10: Reflected intensity I_p measured and estimated using Equation (10) for material C.

sample curvature is known with other parameters required to calculate incident (θ_i) and reflection (θ_r) angles as described in Equation (1).

5. CONCLUSION

In this paper we have presented a measurement setup which can be used to perform gonio-metric measurements of homogenous non-diffuse flexible object materials (for example packaging substrates) using an image based technique at a relatively faster speed. Phong reflection model was used to demonstrate BRDF measurement using the presented setup. Phong model was implemented using two methods (Colour Phong reflection model and Monochrome Phong reflection model).

In the Colour Phong reflection model, object colour was used as the diffuse component I_d of the light source and incident light I_i as the specular component I_s. Phong parameters (k_{amb}, k_d, k_s and α) were estimated using all the three camera sensors (R,G and B). Image data captured using three different incident light directions (θ_L) were used as training data for estimation. Root Mean Square (RMS) error was calculated between the measured and estimated reflected light intensity. The results (refer Table 3 and Figures 6,7, and 8) show that

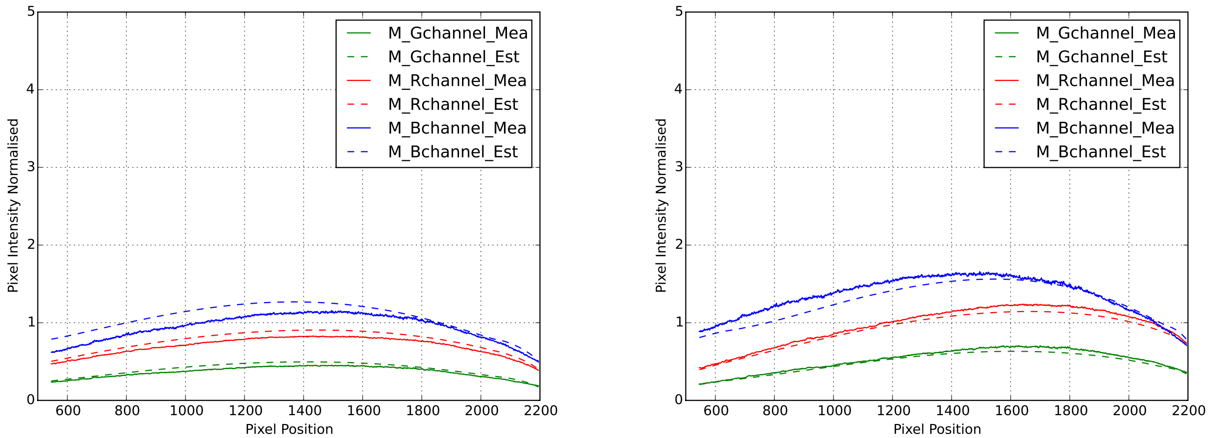

(a) θ_L=29° (b) θ_L=47°

Figure 11: Reflected intensity I_p measured and estimated using Equation (10) for material M.

Table 4: Phong model parameters fitted using the Monochrome Phong reflection model (Section 4.2).

	Sensor channels	**ka**	**kd**	**ks**	**alpha**	**LRMSE**
Material W	**Green**	0.0982	0.4633	0.1719	0.9882	0.0073
	Red	0.2498	0.6093	0.2805	1.0204	0.0681
	Blue	0.3115	1.4458	0.7364	1.0624	0.0907
Material C	**Green**	0.1704	0.474	0.3072	1.124	0.0498
	Red	0.0746	0.1494	0.1345	1.2157	0.0185
	Blue	0.4371	0.6363	0.8319	1.0734	0.0979
Material M	**Green**	0.0727	0.1811	0.1543	1.2918	0.0203
	Red	0.1853	0.4019	0.2114	1.1212	0.0489
	Blue	0.235	0.0416	0.4305	1.2728	0.0377

the measurement setup and the Phong reflection model works well to estimate the BRDF of the sample material used. To compare and evaluate the performance of the measurement setup it would be ideal to measure these sample materials with a gonio-spectrophotometer and evaluate the performance of setup presented above against these measurements. Due to limited access to such an instrument this evaluation could not be performed in this paper.

In the Monochrome Phong reflection model, we have used the incident light I_i as both the diffuse light component and the specular light component in the Phong reflection model. Also, the material image being captured using three sensors (R, G and B), the Phong parameters were estimated separately for R, G and B intensities for the respective sample material. Modelling the Phong parameters for individual sensors and using the incident light as the diffuse and specular light component, in the model, the material appearance could be simulated using the incoming light information. This approach should specifically help simulate/visualise material appearance for highly non-diffuse and gonio-chromatic homogenous materials. Similar to first method, RMS error was calculated between the measured and estimated reflected light intensity. The results (refer Table 4 and Figures 9,10, and 11) show that thought the RMS values are high (especially for blue sensor channel), which may be due to the fluorescence in the sample material used),the measurement setup and the Phong reflection model can be used to estimate the sensor dependent BRDF of the sample material used in this paper.

ACKNOWLEDGMENTS

We would like to thank and acknowledge the support of Dr. Peter Nussbaum from the Norwegian Colour and Visual Computing Laboratory, Gjøvik University College, Norway and Mr. Johansson Niklas from Digital Print Center, Mid Sweden University, Sweden for there participation in discussions. We would also like to thank Mr. Ping Zhao from the Norwegian Colour and Visual Computing Laboratory, Gjøvik University College, Norway for discussions on camera characterisation.

REFERENCES

1. S. R. Marschner, S. H. Westin, E. P. F. Lafortune, K. E. Torrance, and D. P. Greenberg, "Image-based brdf measurement including human skin," in *10th Eurographics Workshop on Rendering*, pp. 139 – 152, 1999.
2. C. S. McCamy, "Observation and measurement of the appearance of metallic materials. part 1. macro appearance." Journal, 1996.
3. K. Kehren, *Optical Properties and Visual Appearance of Printed Special Effect Colors.* PhD thesis, Technischen Universität Darmstadt, Darmstadt, Germany, April 2013.
4. *Appearance Measurements of Goniochromatic Colours*, (Edinburgh, UK), 3rd International Conference on Appearance, April 2012.
5. M. Neuman, P. Edström, M. Andersson, L. G. Coppel, and O. Norberg, "Angular variations of color in turbid media - the influence of bulk scattering on goniochromism in paper," pp. 407 – 413, 2010.
6. M. Neuman and P. Edström, "Anisotropic reflectance from turbid media. ii measurements," *Journal of Optical Society, America* **27**, pp. 1040–1045, 2010.
7. C. S. McCamy, "Observation and measurement of the appearance of metallic materials. part ii. micro appearance," 1998.
8. G. Baba, "Gonio-spectrophotometry of metal-flake and pearl-mica pigmented paint surfaces," in *Proceedings of the fourth Oxford conference on spectrophotometry*, pp. 79–86, SPIE, 2003.
9. J. J. K. Rong Lu and A. M. L. Kappers, "Optical properties (bidirectional reflection distribution functions) of velvet," *Applied Optics* **37**, pp. 5974 – 5984, September 1998.
10. A. Jonathan, A. P., and H. Heo, "A micro-goniophotometer and the measurement of print gloss," *Journal of Imaging and Science Technology* **48**(5), pp. 458 – 463, 2004.
11. S. Tominaga and N. Tanaka, "Estimating reflection parameters from a single color image," *IEEE Computer Graphics and Applications* **20**(5), pp. 58 – 66, 2000.
12. A. Sole, I. Farup, and S. Tominaga, "An image based multi-angle method for estimating reflection geometries of flexible objects," *Color and Imaging Conference* **2014**, pp. 91–96, Novemeber 2014-11-03T00:00:00.
13. F. E. Nicodemus, J. Richmond, J. J. Hsia, I. W. Ginsberg, and T. Limperis, "Geometrical considerations and nomenclature for reflectance." National Bureau of Standards, 1977.
14. B. T. Phong, "Illumination for computer generated pictures," *Commun. ACM* **18**, pp. 311–317, June 1975.
15. J. F. Blinn, "Models of light reflection for computer synthesized pictures," in *Proceedings of the 4th Annual Conference on Computer Graphics and Interactive Techniques, SIGGRAPH '77*, pp. 192–198, ACM, (New York, NY, USA), 1977.
16. R. L. Cook and K. E. Torrance, "A reflectance model for computer graphics," *ACM Trans. Graph.* **1**, pp. 7–24, Jan. 1982.
17. S. Tominaga, "Dichromatic reflection models for rendering object surfaces," *Journal of Imaging Science and Technology* **40**(6), pp. 549 – 555, 1996.
18. N. J. A and R. Mead, "A simplex method for function minimization," *The Computer Journal* **7**, pp. 308 – 313, January 1965.